PERGAMON

Journal of Structural Geology 25 (2003) 841–854

JOURNAL OF STRUCTURAL GEOLOGY

www.elsevier.com/locate/jsg

2-D shape preferred orientations of rigid particles in transtensional viscous flow

Fernando O. Marques[a,*], Sara Coelho[b]

[a]CGUL, Faculdade de Ciências, Univ. Lisboa, Edifício C8, Piso 6, 1749-016 Lisboa, Portugal
[b]Faculdade de Ciências, Univ. Lisboa, Edifício C4, Piso 1, 1749-016 Lisboa, Portugal

Received 16 December 2001; received in revised form 17 June 2002; accepted 28 June 2002

Abstract

Ghosh and Ramberg [Tectonophysics 34 (1976) 1–70] studied the two-dimensional (2-D) rotational behaviour of individual rigid particles embedded in a viscous medium subject to simple shear and transpression ($S_r > 0$), at low/medium shear strains. We now extend this theoretical study to transtension ($S_r < 0$) by deriving a new analytical solution, to non-interacting populations of rigid particles and to high shear strains. We used different initial orientations of particles in the same graph to simulate populations of particles in an originally isotropic rock. Our results show that: (1) shape preferred orientations (SPOs) developed in viscous simple shear flow are transient and cyclical, except for particles with aspect ratio = ∞ (or material lines), which tend to the shear direction; (2) stable SPOs can develop in transpression; they dip towards the shear sense but, when defining an S/C structure with the shear foliation, this composite fabric is always antithetic and, thus, indicates the wrong sense of shear; (3) stable SPOs can also develop in transtension; they dip opposite to the shear sense but, when defining an S/C structure with the shear foliation, this composite fabric is always synthetic and, thus, indicates the correct sense of shear; (4) SPOs produced in transpression or transtension can be used as vorticity gauges only when they represent stable orientations, which must be demonstrated a priori.

Keywords: Theoretical modelling; Rotation; Rigid particles; Shape preferred orientation (SPO); Transtension

1. Introduction

Many are the situations in nature in which rigid particles rotate within viscous fluids and can develop a shape preferred orientation (SPO). This is the case for magmatic flow (either intrusive or extrusive), flow in ductile shear zones and flow in sedimentary processes. For instance, ductile high-shear strain zones typically comprise porphyroclasts embedded in a finally recrystallized matrix. If flow inside them were simple shear, if Jeffery's (1922) theory were directly applicable and if channelling problems did not take place (Marques and Coelho, 2001), then all porphyroclasts would show signs of rotation: (1) if metamorphic conditions allowed formation of recrystallization tails, then shear zones would be dominated by rolling structures (Van den Driessche and Brun, 1987) and/or by δ structures (Passchier and Simpson, 1986); (2) if tails did not form, signs of synthetic rotation of clasts should be observed in the surrounding shear foliated and ductile matrix (e.g. Ghosh and Ramberg, 1976; Arbaret et al., 2001 and drag folds of Rosas et al., 2002). Why, then, are rolling structures not so common in many known ductile shear zones? Possible answers to this question are: (1) the flow inside the shear zone is an association of pure shear and simple shear, with compression normal to the shear direction (2-D transpression; Fig. 1A). The pure shear component can inhibit rotation of the particles as shown by Ghosh and Ramberg (1976) (see also Bretherton, 1962; Gay, 1968; Willis, 1977; Freeman, 1985; Ježek, 1994; Ježek et al., 1994, 1996). (2) The flow inside the shear zone is confined. If the ratio between particle least axis and width of shear zone is small, synthetic rotation can be inhibited, and even antithetic rotation beyond the shear plane is possible (Marques and Coelho, 2001). (3) A slipping matrix/particle interface (Ildefonse and Mancktelow, 1993; Marques and Cobbold, 1995; Marques and Coelho, 2001). The experimental work of Ildefonse and Mancktelow (1993) showed that a

* Corresponding author. Tel.: +351-217-500000; fax: +351-217-500064.
E-mail address: fmarques@fc.ul.pt (F.O. Marques).

0191-8141/03/$ - see front matter
PII: S0191-8141(02)00089-5

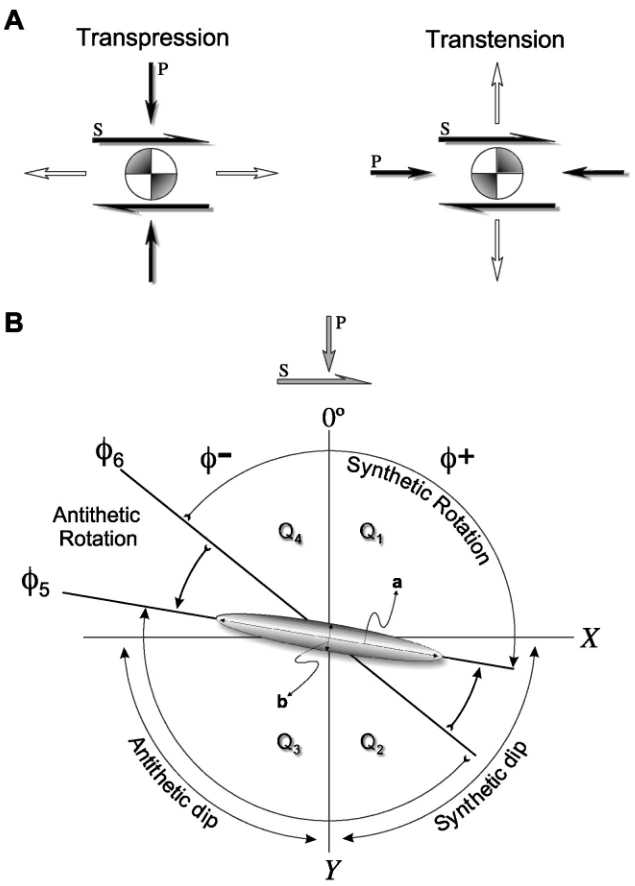

Fig. 1. Schematic representation of reference frames and angles used in the text. (A) 2-D transpression and 2-D transtension with arrows indicating the simple shear (S) and pure shear (P) components. Shaded areas represent quadrants where stable and metastable positions are possible. (B) X is parallel to the shear direction of the simple shear component and to compression of the pure shear component in transtension, and Y is parallel to compression of the pure shear component in transpression. The angle of rotation (ϕ) of particles is measured from Y and is positive clockwise in dextral simple shear. ϕ_5 represents a stable orientation and ϕ_6 a metastable orientation. a and b are the principal axes of the particle, and its aspect ratio (R) equal to a/b. Quadrants 1–4 are represented by Q_n.

slipping interface induces a slower rotation, and suggests that the inclusion tends to stabilise with its longest axis parallel to the shear plane (they worked at low shear strains and thus extrapolations to higher strains are not applicable) (see also Arbaret et al., 2001). (4) The flow inside the shear zone is an association of pure shear and simple shear, with compression parallel to the shear direction (2-D transtension; Fig. 1A). Again, the pure shear component can inhibit rotation of the particles, as we will show in the present study.

Ghosh and Ramberg (1976) (see also Reed and Tryggvason, 1974) investigated the 2-D rotation of single particles, in low shear strain intervals, in simple shear and transpression ($S_r > 0$). We now extend their theoretical work to transtension ($S_r < 0$), to high shear strains ($\gamma > 10$) and to populations of non-interacting particles. This allows the investigation of: (1) new stable orientations; (2) SPOs; (3) the behaviour of composite structures (like S/C) with progressive shear strain, and their use as criteria for the determination of shear sense; (4) vorticity gauges. The results are valid for plane strain, i.e. with no extension or contraction along the direction of the vorticity vector.

Ildefonse and Fernandez (1988) and Ildefonse et al. (1992a,b) investigated the rotational behaviour of populations of interacting rigid particles (dense suspensions) at low shear strains. We now investigate the rotational behaviour of populations of non-interacting rigid particles in a wide range of shear strains. It is also not the aim of the present work to investigate the effect of particle shapes on the rotational behaviour of rigid particles as done by Willis (1977) and Fernandez et al. (1983).

The concentration/dispersion of orientation of particles can be qualitatively evaluated from observation of convergence/divergence of curves in the graphs presented in this study. However, for a quantitative evaluation, we added to some of the graphs the curve that reflects the intensity of the fabric, i.e. the percentage of particles that define the SPO. Maximum concentration is given by 100% (all particles have identical orientation) and maximum dispersion is given by 0%.

2. 2-D rotation of rigid particles in a viscous matrix

Based on Jeffery's (1922) theory, Ghosh and Ramberg (1976) derived the equations for the 2-D rotation of elliptical rigid particles embedded in a viscous matrix subjected to simple shear or to a combination of pure and simple shear (2-D transpression). They showed that reorientation depends on the ratio between the rates of pure and simple shear components ($S_r = \dot{\epsilon}/\dot{\gamma}$), on particle's orientation (the angle of the particle's longest axis with the normal to the shear direction—ϕ) and on particle's aspect ratio ($R = a/b$; Fig. 1B). When $S_r = 0$ flow is simple shear and when $S_r = \infty$ flow is pure shear. $\phi = 0°$ when the particle's long axis is parallel to Y and $\phi = 90°$ when parallel to the shear direction (X). Positive angles are measured clockwise (Fig. 1B) from $\phi = 0°$ and considered synthetic in top to the right sense of shear. The rate of rotation of rigid elliptical particles by a simultaneous combination of simple and pure shear is given by equations 3 and 4 of Ghosh and Ramberg (1976) and equation 5 of Ghosh (1977):

$$\dot{\phi} = \frac{\dot{\gamma}(R^2\cos^2\phi + \sin^2\phi)}{R^2+1} + \frac{\dot{\epsilon}_x(R^2-1)\sin 2\phi}{R^2+1}$$

whose solutions show that: (1) inclusions rotate at different angular velocities depending on ϕ, with the exception of inclusions with $R = 1$, which rotate continuously and at a constant rate given by $\dot{\gamma}/2$; (2) for each S_r value there is a

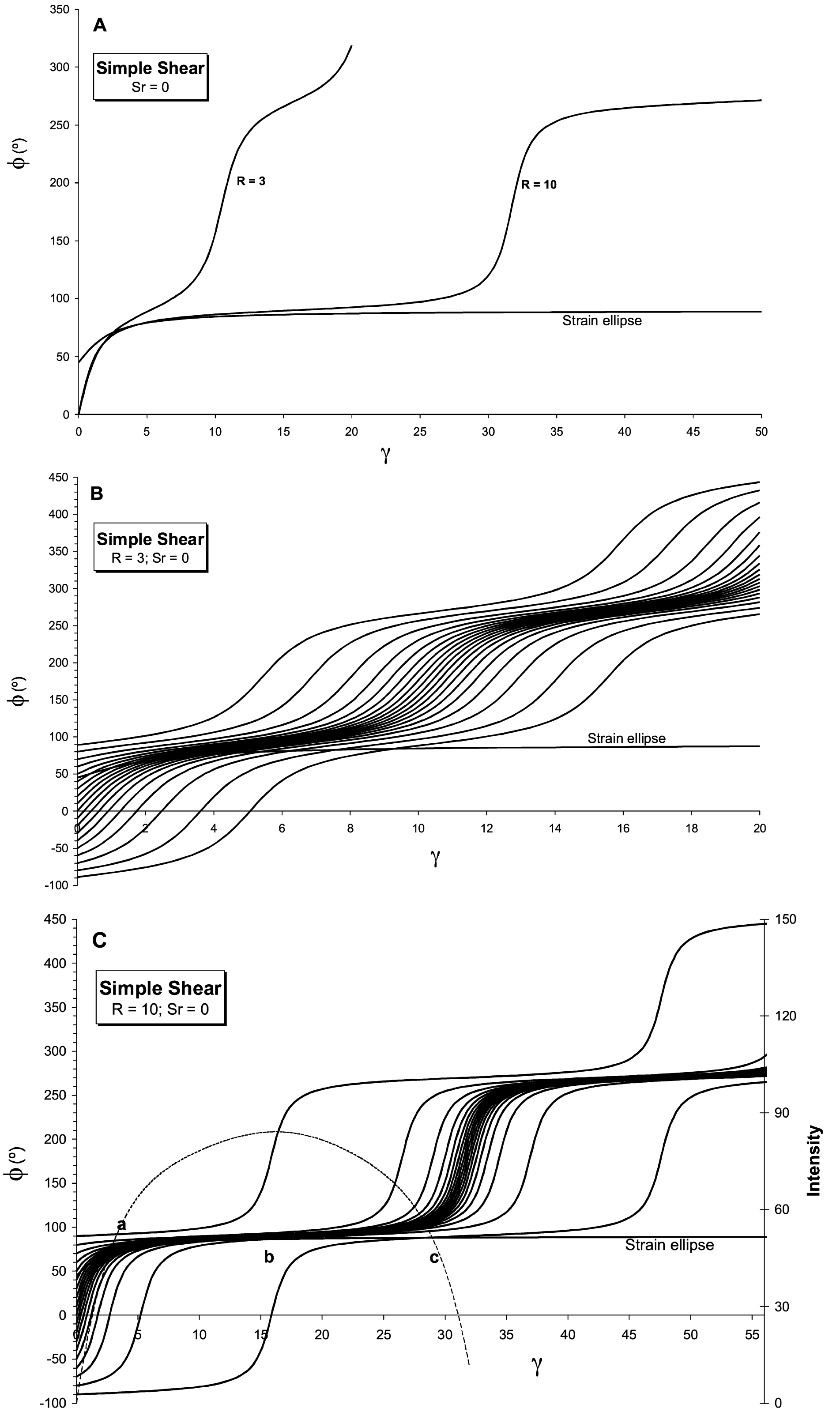

Fig. 2. (A) Graph illustrating the cyclic character of particle rotation and variation of 'ramp/flat' geometry depending on R and shear strain. Rotation of the greatest axis of the strain ellipse is also added for comparison. (B) and (C) Analytical solutions for rotation of populations of particles with $R = 3$ and $R = 10$, respectively, starting at different ϕ_i. (C) From (A) to (B), i.e. during approximately 12 γ, there is a synthetic C/S fabric that fades away towards (B). From (B) to (C) (again 12 γ), an antithetic C/S fabric slowly develops. At ca. 31 γ, a new cycle begins. The intensity curve was added (dashed) for a quantitative evaluation of dispersion of particle orientations.

critical aspect ratio (R_{crit}), given by:

$$R_{\mathrm{crit}} = \frac{1+\sqrt{1+4S_{\mathrm{r}}^2}}{2S_{\mathrm{r}}}$$

which defines the way particles rotate. If $R > R_{\mathrm{crit}}$, rotation stops at a stable orientation (ϕ_5 of Ghosh and Ramberg, 1976, equation 8b):

$$\phi_5 = \tan^{-1}\left[-S_{\mathrm{r}}\left(R^2-1\right) - \sqrt{S_{\mathrm{r}}^2(R^2-1)^2 - R^2}\right]$$

which is equivalent to a sink or fabric attractor as defined by Passchier (1987, 1997). There is also a metastable orientation, the ϕ_6 of Ghosh and Ramberg (1976); if $R < R_{\mathrm{crit}}$, the particle rotates continuously and synthetically. In simple shear $R_{\mathrm{crit}} = \infty$ and, thus, natural rigid inclusions rotate continuously and synthetically. This means that there is no fabric attractor for such rigid inclusions in simple shear.

2.1. Reorientation of rigid particles in viscous simple shear

To better understand the behaviour of individual particles and to study the 2-D fabrics that can develop by rotation of non-interacting populations of rigid particles in viscous simple shear, we expanded graphs 5 and 6 of Ghosh and Ramberg (1976) to higher γ and to different initial orientations (to simulate populations of particles), with different values of R (3 and 10) (Fig. 2), by using their equation 12, because there are no stable orientations.

Analysis of graphs for $R = 3$ and $R = 10$ (Fig. 2B and C) shows that: (1) SPO defined by longest axes of rigid particles develops cyclically; (2) the SPO lasts for longer for $R = 10$; (3) a closer look at the graph for $R = 10$ (Fig. 2C) reveals that: (i) in *a* ($\gamma \approx 3$), a conspicuous SPO is developed due to reorientation of most particles at a ϕ of ca. 70–80° (antithetic dip of 10–20° with the shear direction; see Fig. 1B), which can be enhanced by plastically deforming minerals (coincident with e_1 of the finite strain ellipse); (ii) from *a* to *b*, the SPO becomes more intense and slowly tends to the shear direction; (iii) in *b* ($\gamma \approx 16$) the SPO is statistically parallel to the shear direction; (iv) from *b* to *c* ($\gamma \approx 29$) the SPO becomes less intense and slowly moves away from the shear direction.

2.2. Reorientation of rigid particles in viscous transpression

2-D transpression is a combination of pure shear and simple shear, with compression of pure shear component normal to shear direction (Ghosh and Ramberg, 1976) (Fig. 1A) and $S_{\mathrm{r}} > 0$. We used their equation 12 when $B^2 < AC$, and their equation 11 when $B^2 > AC$ (see Section 2.3). The major difference between transpression and simple shear is that, for the former, there are stable orientations (ϕ_5) for particles with $R_{\mathrm{crit}} < R < \infty$.

2.2.1. $R = 3$ and variable S_r

For $S_{\mathrm{r}} = 0.1$, 0.25 and 1.0, $R_{\mathrm{crit}} = 10.10$, 4.24 and 1.62, respectively. Thus, particles with $R = 3$ rotate continuously and synthetically for $S_{\mathrm{r}} = 0.1$ and 0.25, and have a ϕ_5 for $S_{\mathrm{r}} = 1.0$. For $R = 3$ and $S_{\mathrm{r}} = 0.1$ (equation 12 of Ghosh and Ramberg, 1976) (Fig. 3A), a fairly intense SPO is produced only by particles with ϕ_i between −40° and 60°. This fabric lasts for about 6 γ, with variable sense of dip relative to the shear direction, but mostly synthetic, before particles spread apart and enter a new cycle. For $R = 3$ and $S_{\mathrm{r}} = 0.25$ (equation 12 of Ghosh and Ramberg, 1976) (Fig. 3B), an intense fabric is produced by particles with ϕ_i between −50° and 80°. The SPO lasts for about 10 γ, with a synthetic dip, before particles spread apart and enter a new cycle. For $R = 3$ and $S_{\mathrm{r}} = 1.0$ (equation 11 of Ghosh and Ramberg, 1976) (Fig. 3C) all particles tend to a stable orientation with a synthetic dip of about 4° with the shear direction. Antithetic rotation takes place for particles with ϕ_i between −30.2° and −86.3°.

2.2.2. $R = 10$ and variable S_r

For $S_{\mathrm{r}} = 0.1$, 0.25 and 1.0, $R_{\mathrm{crit}} = 10.10$, 4.24 and 1.62, respectively. Thus, particles with $R = 10$ rotate continuously and synthetically for $S_{\mathrm{r}} = 0.1$, and have a ϕ_5 for $S_{\mathrm{r}} = 0.25$ and 1.0. For $R = 10$ and $S_{\mathrm{r}} = 0.1$ (equation 12 of Ghosh and Ramberg, 1976) (Fig. 4A) an intense SPO is produced by particles with ϕ_i between −60° and 90°. The SPO can last for about 200 γ, with a synthetic dip (except for the very initial stage of a cycle; Fig. 4A), before particles spread apart and enter a new cycle. For $R = 10$ and $S_{\mathrm{r}} = 0.25$ (equation 11 of Ghosh and Ramberg, 1976) (Fig. 4B) all particles tend to a stable orientation with a synthetic dip of about 1.2° with the shear direction. For $R = 10$ and $S_{\mathrm{r}} = 1.0$ (equation 11 of Ghosh and Ramberg, 1976) (Fig. 4C) all particles tend to a stable orientation with a synthetic dip of about 0.3° with the shear direction.

Analysis of graphs for $R = 3$ and $R = 10$, in transpression (Figs. 3 and 4, respectively), shows that: (1) when there is no ϕ_5, SPOs can be intense but are transient; (2) for identical R, the transient SPO lasts for longer for higher values of S_{r}; (3) transient SPOs are more intense and last for longer for $R = 10$ than for $R = 3$, at identical S_{r}; (4) the greater the R and S_{r}, the more intense the SPO, its orientation being very close to the shear direction. However, measuring such angles in natural rocks would be virtually impossible; (5) when there is a ϕ_5, the most intense SPO is developed early in deformation, especially if R and S_{r} are reasonably high; (6) Stable positions, and most transient SPOs in 2-D transpression dip synthetically, and can, therefore, give rise to antithetic composite fabrics like S/C fabrics.

2.3. Reorientation of rigid particles in viscous transtension

Transtension is here considered a 2-D combination of

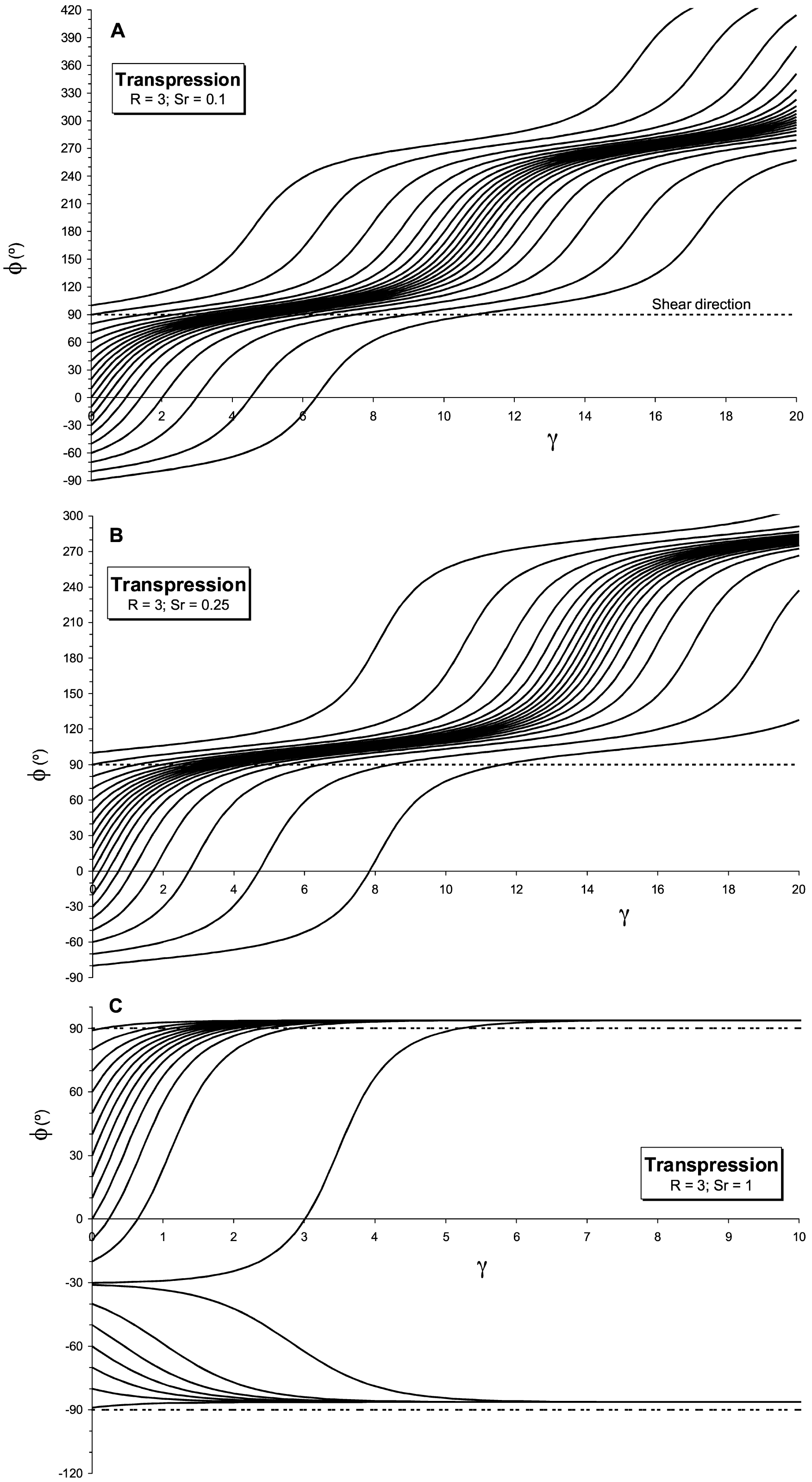

Fig. 3. Analytical solutions for rotation of particles in transpression, with $R = 3$ and $S_r = 0.1$ (A), 0.25 (B) and 1.0 (C), starting at different ϕ_i. Note that: (i) ϕ_5 only exists for $S_r = 1.0$; (ii) duration of the SPO in (A) and (B) is directly dependent on S_r; (iii) there is back rotation in (C), for particles with ϕ_i between $-30.2°$ and $-86.3°$.

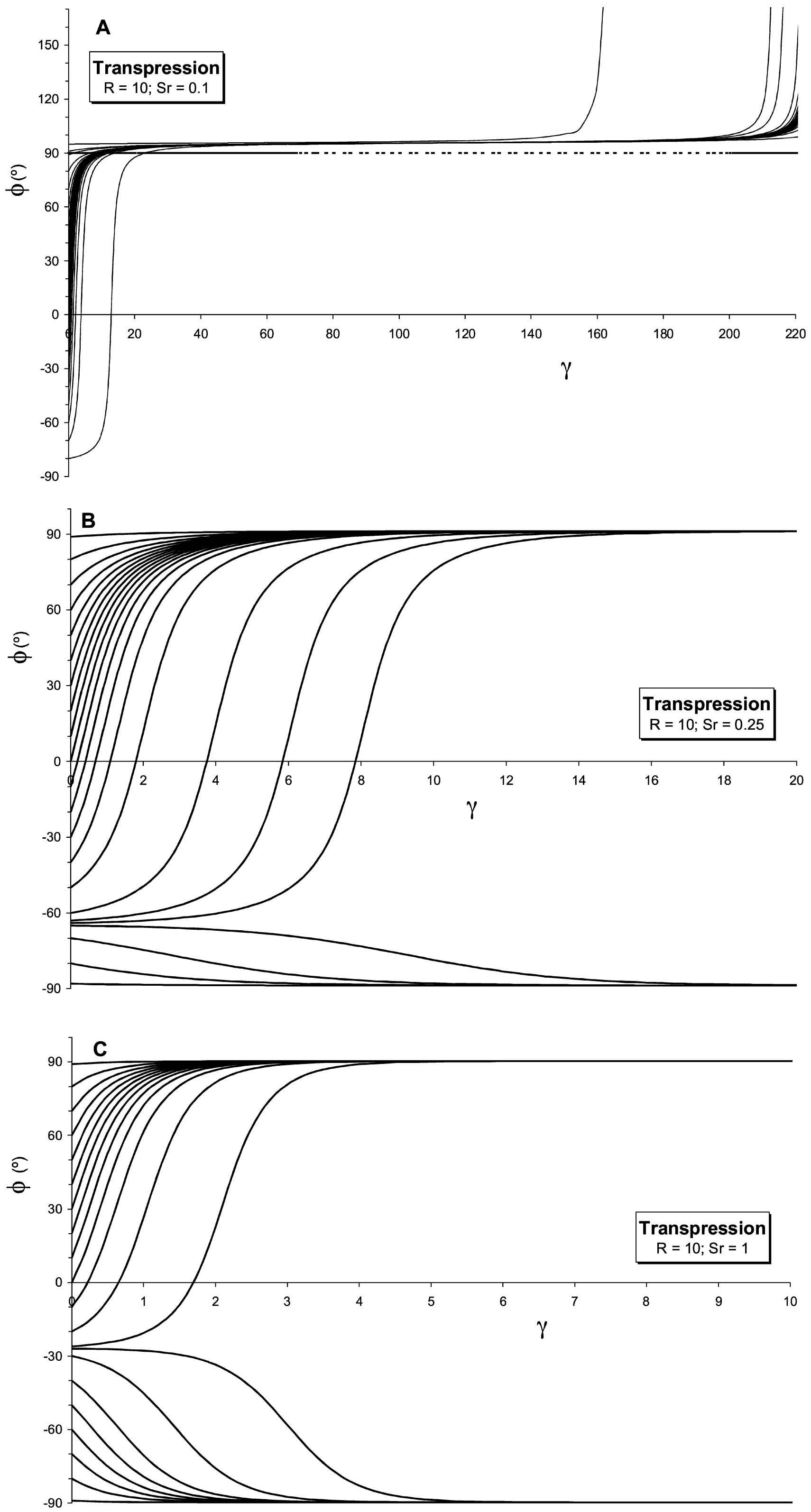

Fig. 4. Analytical solutions for rotation of particles in transpression, with $R = 10$ and $S_r = 0.1$ (A), 0.25 (B) and 1.0 (C), starting at different ϕ_i. Note that: (i) ϕ_5 exists for $S_r = 0.25$ and 1.0; (ii) duration of the SPO in (A) is much greater than in Fig. 3A and B, showing direct dependence on R; (iii) there is back rotation in (B) and (C), for different intervals of ϕ_i.

pure and simple shear, with compression of pure shear component parallel to the shear direction (Fig. 1A) and $S_r < 0$. Ghosh and Ramberg (1976) derived the equations for the rate of rotation of inclusions in 2-D transpression by adding the rotation rates of simple and pure shear (their equations 1 and 2, respectively). In 2-D transtension, the rate of pure shear is negative because of opposite sense of the pure shear component relative to 2-D transpression (Fig. 1A). Then, equation 3 of Ghosh and Ramberg (1976):

$$\dot{\phi} = \frac{\dot{\gamma}(R^2\cos^2\phi + \sin^2\phi)}{R^2+1} + \frac{\dot{\epsilon}_x(R^2-1)\sin 2\phi}{R^2+1}$$

becomes:

$$\dot{\phi} = \frac{\dot{\gamma}(R^2\cos^2\phi + \sin^2\phi)}{R^2+1} - \frac{\dot{\epsilon}_x(R^2-1)\sin 2\phi}{R^2+1}$$

Their equation 12:

$$\phi = \tan^{-1}\left[\frac{\sqrt{AC-B^2}}{C}\tan\left\{\gamma\sqrt{AC-B^2} + \tan^{-1}\left(\frac{C\tan\phi_0 + B}{\sqrt{AC-B^2}}\right)\right\} - \frac{B}{C}\right]$$

becomes:

$$\phi = \tan^{-1}\left[\frac{\sqrt{AC-(-B)^2}}{C}\tan\left\{\gamma\sqrt{AC-(-B)^2} + \tan^{-1}\left(\frac{C\tan\phi_0 + (-B)}{\sqrt{AC-(-B)^2}}\right)\right\} - \frac{(-B)}{C}\right]$$

where:

$$A = \frac{R^2}{R^2+1};$$

$$B = \frac{S_R(R^2-1)}{R^2+1}$$

and

$$C = \frac{1}{R^2+1}.$$

Equation 11 of Ghosh and Ramberg (1976):

$$\phi = \tan^{-1}\frac{P\left(B+\sqrt{B^2-AC}\right) - B + \sqrt{B^2-AC}}{C(1-P)}$$

becomes:

$$\phi = \tan^{-1}\frac{P\left(-B+\sqrt{B^2-AC}\right) + B + \sqrt{B^2-AC}}{C(1-P)},$$

where

$$P = \frac{C\tan\phi_0 - B - \sqrt{B^2-AC}}{C\tan\phi_0 - B + \sqrt{B^2-AC}}\exp\left(2\gamma\sqrt{B^2-AC}\right)$$

because B is a function of S_r, which changes sign in transtension.

2.3.1. $R = 3$ and variable S_r

For $S_r = -0.1$, -0.25 and -1.0, $R_{crit} = 10.10$, 4.24 and 1.62, respectively. Thus, particles with $R = 3$ rotate continuously and synthetically for $S_r = -0.1$ and -0.25, and have a ϕ_5 for $S_r = -1.0$. For $R = 3$ and $S_r = -0.1$ (Fig. 5A) a fairly intense SPO is produced only by particles with ϕ_i between $-40°$ and 50°. This fabric lasts for about 6 γ, with variable sense of dip relative to the shear direction but mostly antithetic, before particles spread apart and enter a new cycle. For $R = 3$ and $S_r = -0.25$ (Fig. 5B), a fairly intense fabric is produced by particles with ϕ_i between 50° and $-60°$. The SPO lasts for about 10 γ, with an antithetic dip, before particles spread apart and enter a new cycle. For $R = 3$ and $S_r = -1.0$ (Fig. 5C) all particles tend to a stable orientation with an antithetic dip of about 60° with the shear direction, defining an SPO at low values of shear strain ($\gamma = 2$). Antithetic rotation takes place for particles with ϕ_i between 30.2° and 86.3°.

2.3.2. $R = 10$ and variable S_r

For $S_r = -0.1$, -0.25 and -1.0, $R_{crit} = 10.10$, 4.24 and 1.62, respectively. Thus, particles with $R = 10$ rotate continuously and synthetically for $S_r = -0.1$, and have a ϕ_5 for $S_r = -0.25$ and -1.0. For $R = 10$ and $S_r = -0.1$ (Fig. 6A) a very intense SPO is produced early in deformation by particles with ϕ_i between $-60°$ and 70°. The SPO can last for more than 200 γ, with an antithetic dip (except for the very final stages of a cycle), before particles spread apart and enter a new cycle. For $R = 10$ and $S_r = -0.25$ (Fig. 6B) all particles tend to a stable orientation with an antithetic dip of about 25° with the shear direction. For $R = 10$ and $S_r = -1.0$ (Fig. 6C) all particles tend to a stable orientation with an antithetic dip of about 63° with the shear direction.

Analysis of graphs for $R = 3$ and $R = 10$, in transtension (Figs. 5 and 6, respectively), shows that: (1) when there is no ϕ_5, SPOs can be intense but are transient; (2) for identical R, the duration of the transient SPO is directly proportional to S_r; (3) transient SPOs are more intense (see values of intensity in graphs of Figs. 5 and 6) and last for longer for $R = 10$ than for $R = 3$, at identical Sr; (4) the greater the R and the absolute value of S_r, the more intense the SPO; (5) when there is a ϕ_5, a very intense SPO is developed early in deformation, especially if R and the absolute value of S_r are reasonably high; (6) the angle between the SPO and the shear direction increases with increasing absolute value of S_r; (7) Stable positions, and most transient SPOs, in 2-D transtension dip antithetically, and can, thus, give rise to synthetic composite fabrics like S/C fabrics.

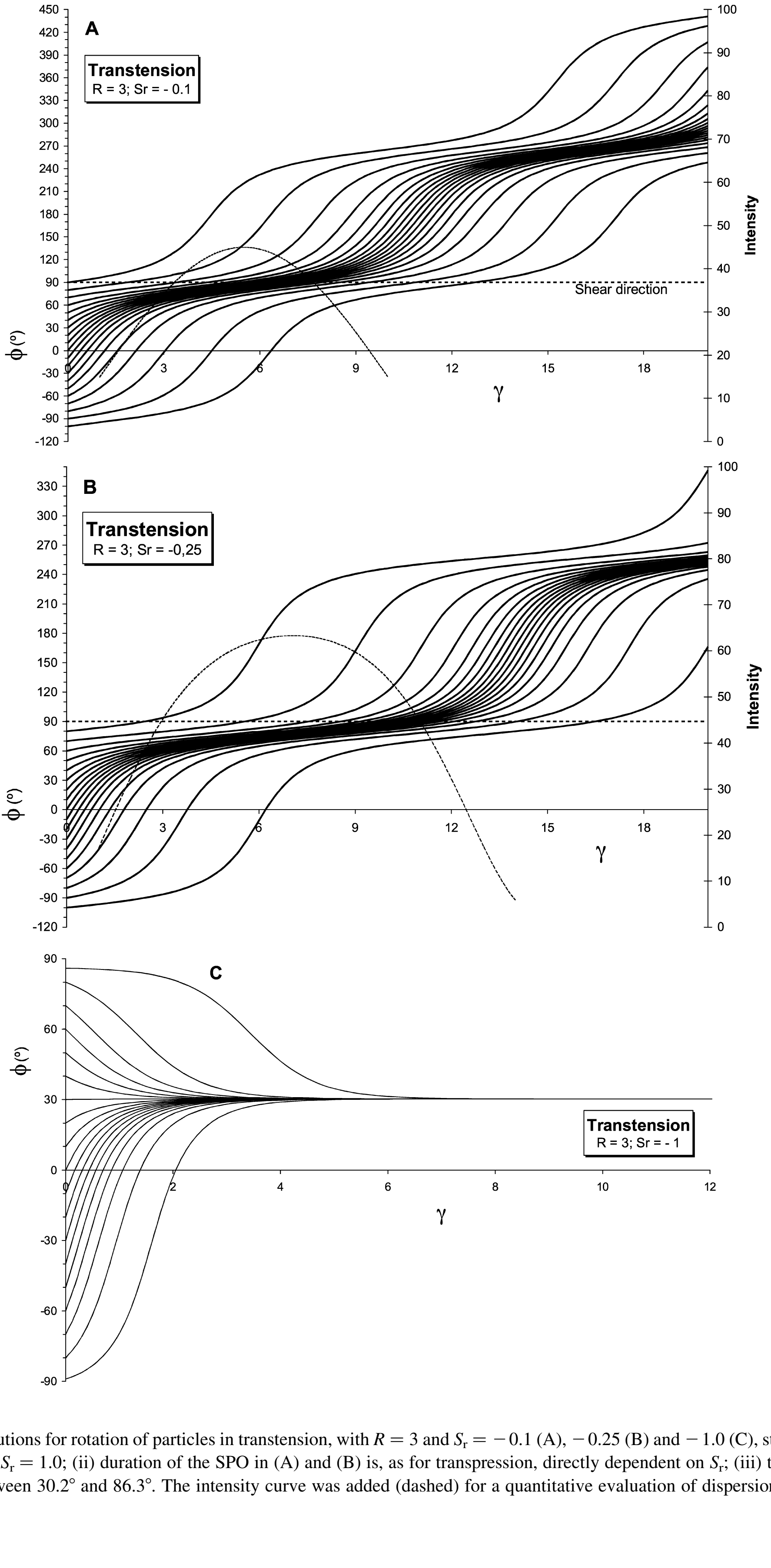

Fig. 5. Analytical solutions for rotation of particles in transtension, with $R = 3$ and $S_r = -0.1$ (A), -0.25 (B) and -1.0 (C), starting at different ϕ_i. Note that: (i) ϕ_5 only exists for $S_r = 1.0$; (ii) duration of the SPO in (A) and (B) is, as for transpression, directly dependent on S_r; (iii) there is back rotation in (C), for particles with ϕ_i between 30.2° and 86.3°. The intensity curve was added (dashed) for a quantitative evaluation of dispersion of particle orientations.

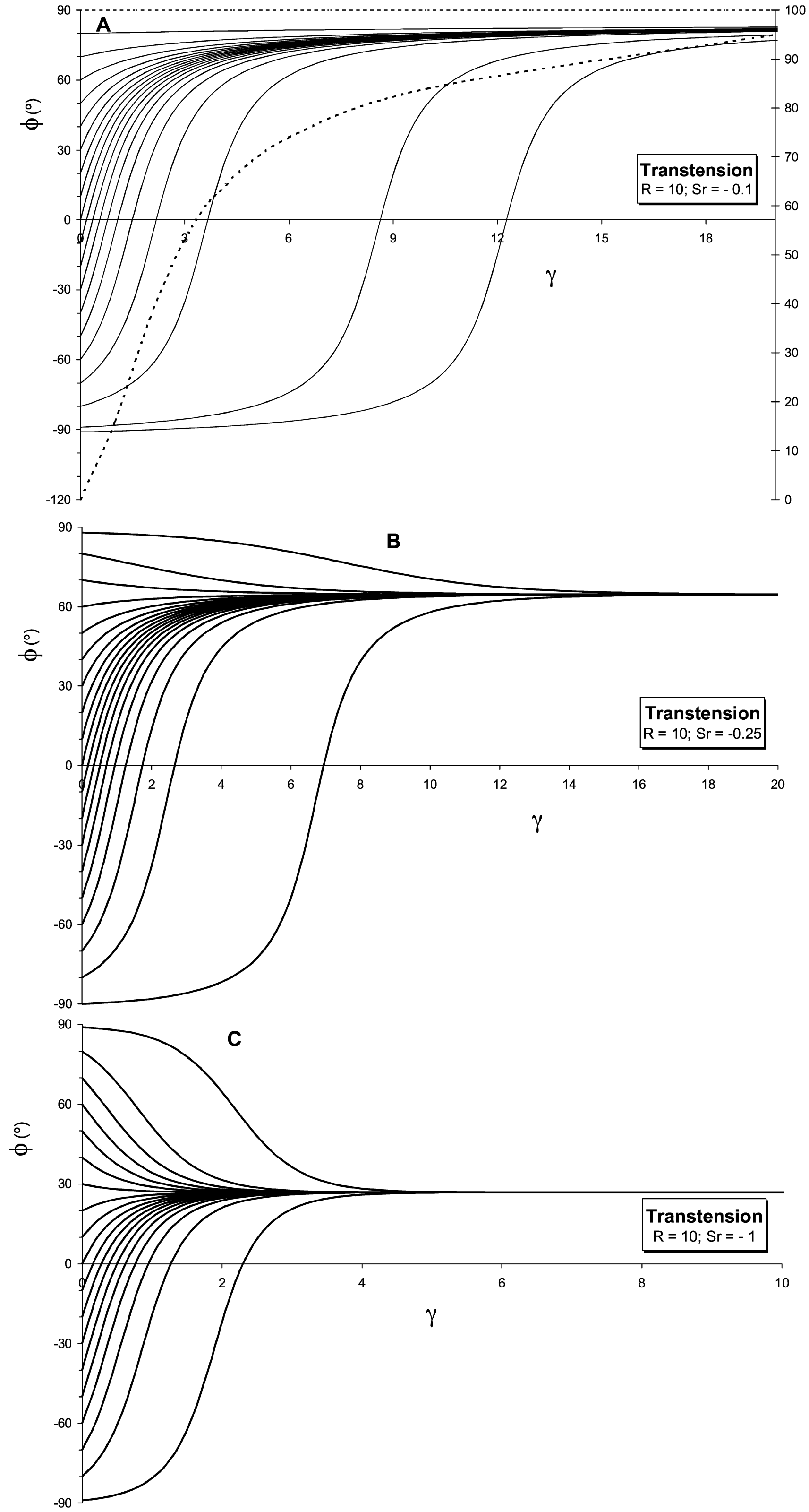

Fig. 6. Analytical solutions for rotation of particles in transtension, with $R = 10$ and $S_r = -0.1$ (A), -0.25 (B) and -1.0 (C), starting at different ϕ_i. Note that: (i) ϕ_5 exists for $S_r = 0.25$ and 1.0; (ii) duration of the SPO in (A) is much greater than in Fig. 5A and B, showing direct dependence on R; (iii) there is back rotation in (B) and (C), for different intervals of ϕ_i. The intensity curve was added (dashed) for a quantitative evaluation of dispersion of particle orientations, and shows that transient SPOs are more intense for $R = 10$ than for $R = 3$, at identical S_r.

3. Discussion

Curves in all shown graphs for simple shear, transpression and transtension are sigmoidal and have two distinct paths: one with a steep slope that indicates fast angular velocity of particles, and another with a flat slope that indicates low angular velocity. This is a consequence of the fact that particles initially favourably oriented (in the steep portion of the curve) rapidly rotate towards a stable or long lasting transient position, and contribute to an intense SPO. Conversely, particles initially unfavourably oriented (in the flat portion of the curve) disturb, more or less significantly, the SPO defined by particles favourably oriented. This holds true for particles that are added to the initial population during deformation.

The graphs of Figs. 7 and 8 show the variations of ϕ_5 with S_r and R, respectively. From the graphs of Figs. 7A and 8A, one can conclude that, in transpression: (i) the greater the R and S_r, the closer the stable orientation becomes to 90°, and the greater the difficulty in distinguishing the SPO from the shear direction; (ii) the greater the R, the smaller the S_r interval in which the SPO can be appreciably far from the shear direction; (iii) the greater the R, the closer the SPO from the shear direction, even at very low S_r. From the graphs of Figs. 7B and 8B, one can conclude that, in transtension: (i) the greater the R and the absolute value of S_r, the further apart the stable orientation becomes from 90°, and the easier the distinction of the SPO from the shear direction; (ii) the greater the R, the greater the S_r interval in which the SPO can be considerably further from the shear direction; (iii) the greater the R, the further apart the SPO from the shear direction, even at very low absolute value of S_r. The graphs of Figs. 7C and 8C show the curves of maximum ϕ_5 for pairs of S_r and R of Figs. 7A and B and 8A and B, respectively. The curves were obtained by making the right term of the ϕ_5 equation equal to zero, in order to find maximum ϕ_5. These curves link the upper tips of curves (at lower R or Sr) in the graphs of Figs. 7A and B and 8A and B, and show that, in transtension, stable SPOs always dip antithetically, conversely to what happens in transpression. The graph of Fig. 9 shows the variation of R with S_r at maximum ϕ_5. This graph shows that the greater the R (or S_r in absolute value), the smaller the absolute value of S_r (or R) needed to get to a maximum angle of stable orientation.

Berthé et al. (1979) give a rather strict definition of S/C structures, a composite fabric in which S stands for *schistosité* and C for *cisaillement*. In our opinion, this definition could have a broader sense and be extended to structures in which there are two planar anisotropies; a shear foliation (C), typical of rocks formed in ductile shear zones, and an oblique foliation (S) formed by the alignment of rotating rigid particles and/or plastically deforming minerals. In this sense, the SPOs studied in the present work can be considered S surfaces at an angle with the shear foliation developed during shear flow (simple shear, transpression or transtension). Comparison of transient SPOs in the three studied flow types shows that: (i) in simple shear, the duration of the synthetic dip is identical to the duration of the antithetic dip, whatever the R value; (ii) in transpression, the duration of the synthetic dip is much longer than the antithetic dip, and depends on the values of R and S_r; and (iii) in transtension, the duration of the antithetic dip is much longer than the synthetic dip, and depends on R and S_r. Therefore, theoretically, in simple shear there is an equal probability of finding a synthetic or an antithetic S fabric formed by rotation of rigid particles. Conversely to simple shear, the composite transient fabric in transpression is always an antithetic S/C-type fabric, which grows stronger until a new cycle begins. On the contrary, the composite transient fabric in transtension is always a synthetic S/C-type fabric, which grows weaker until it vanishes with the beginning of a new cycle. In natural rocks this should be even more realistic, because shear strain of rocks is not infinite, and the first S/C-type fabrics to develop are antithetic in transpression and synthetic in transtension. This particular type of flow (transtension) can well justify the SPO found by Pennacchioni et al. (2001) in the Mount Mary mylonites: an S foliation that defines a synthetic S/C-type fabric with the mylonitic foliation.

The above data and discussion holds true in ideal situations of non-interacting populations of particles, with identical and invariable R, rotating in the plane normal to vorticity (Fig. 1B), and with initial orientations showing a random and anti-clustered distribution (initial isotropic rock). This is certainly not the common case in nature. What can we expect, then, in real rocks? That particles rotate, in particular types of flow, statiscally in the plane normal to the vorticity axis and for high shear strains. This is the case of 3-D transtension (work in progress) with invariant X-direction (shortening parallel to the vorticity axis). What happens if particles have significantly variable values of R? Then, SPOs are not so well defined, because of greater differences in rotation rates and stable orientations. This is particularly true for simple shear, because there are no stable orientations for natural rotating rigid inclusions (R should be equal to infinity).

The natural examples to which the above theory can be applied are mylonites with a fine grain ductile matrix (e.g. quartz, or quartz + fine mica) with embedded competent porphyroclasts with $R > 1$ (e.g. elongated crystals of sillimanite, white mica, feldspar, amphibole). Such a mylonite could derive, by shearing, from a porphyroid granite. A good natural example could be the rocks studied by Pennacchioni et al. (2001).

A great deal of porphyroclasts in a volume of rock (mica-fish for instance), with identical orientation relative to the shear plane, may seem a stable SPO. However, as shown by the graphs with populations of non-interacting particles, such a position can be transient. For instance, in transpression or transtension with $R = 10$ and $S_r = 0.1$, the fabric that develops very early in deformation can last for 200 γ.

The orientation of longest axis and (001) planes of white

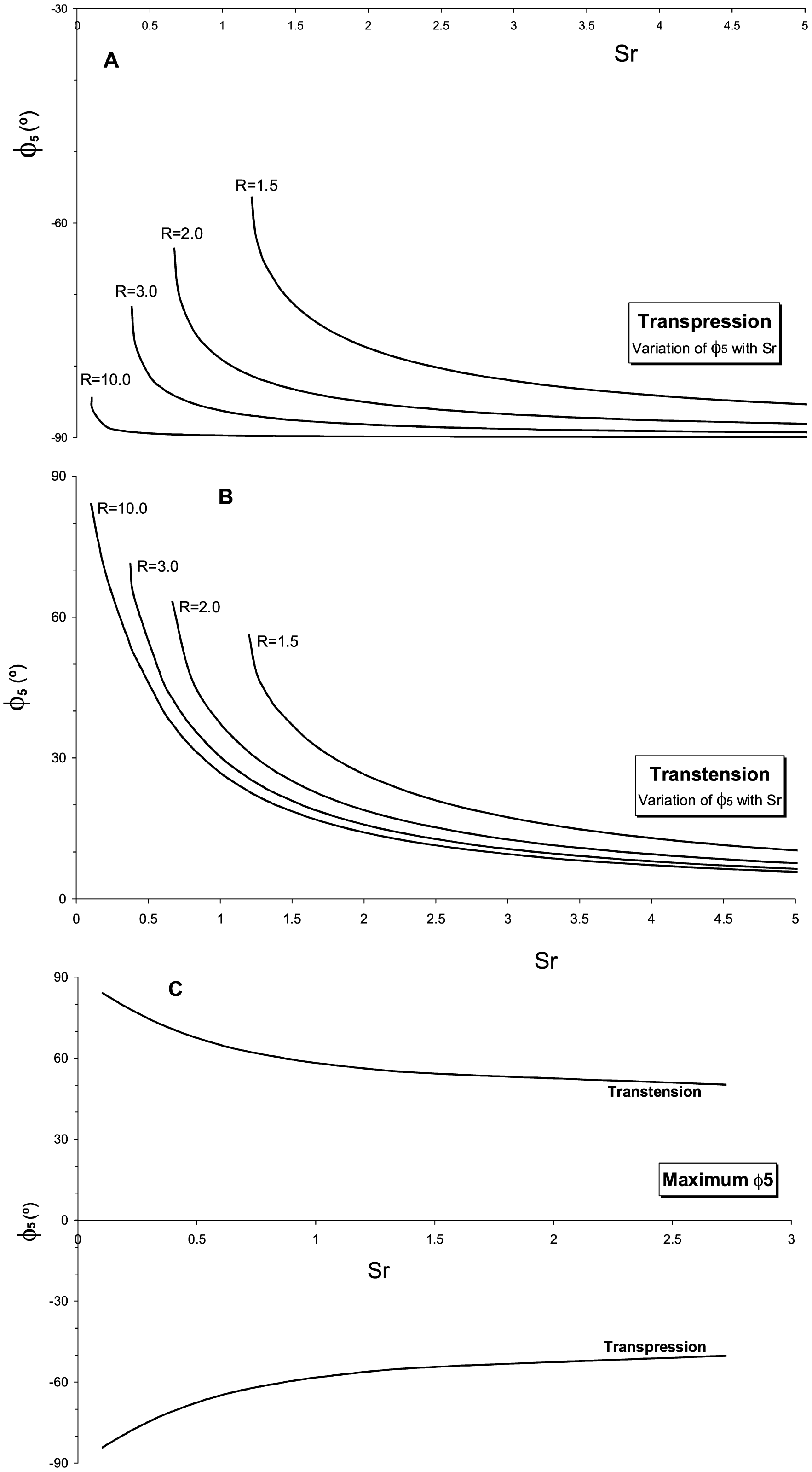

Fig. 7. (A) Graph illustrating the variation of ϕ_5 with S_r, in transpression. (B) Graph illustrating dependence of ϕ_5 on S_r, in transtension. (C) Curves of maximum ϕ_5 for pairs of S_r and R of (A) and (B), respectively. These curves link the upper tips of curves (at lower R or S_r) in the graphs of (A) and (B), and show that, in transtension, stable SPOs always dip antithetically to the shear sense, conversely to what happens in transpression.

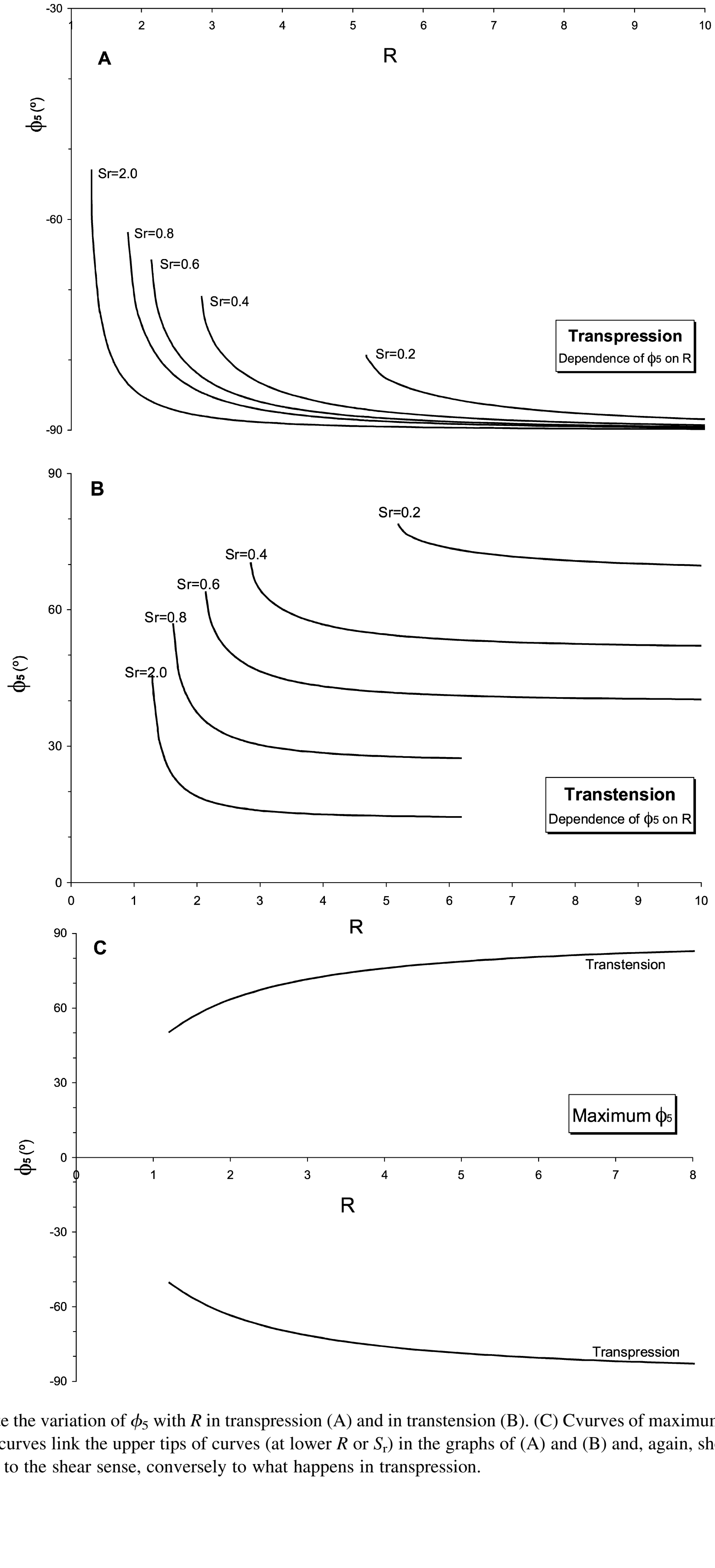

Fig. 8. Graphs to illustrate the variation of ϕ_5 with R in transpression (A) and in transtension (B). (C) Cvurves of maximum ϕ_5 for pairs of S_r and R of (A) and (B), respectively. These curves link the upper tips of curves (at lower R or S_r) in the graphs of (A) and (B) and, again, show that, in transtension, stable SPO always dip antithetically to the shear sense, conversely to what happens in transpression.

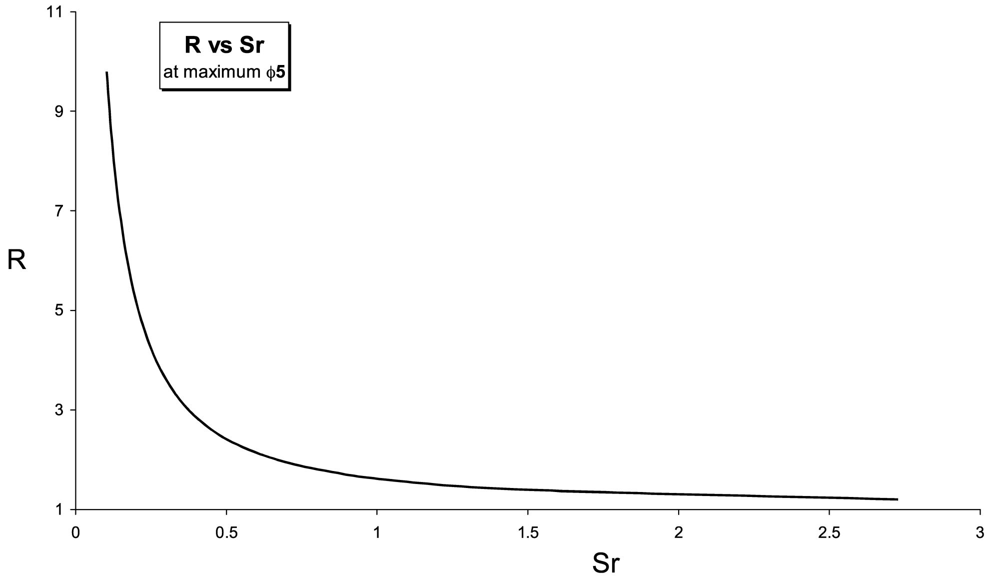

Fig. 9. Graph to show the variation of R with S_r at maximum ϕ_5.

mica oblique to the shear plane is a common feature in mica-rich quartz–feldspar mylonites, which is known as mica-fish. Following Ghosh and Ramberg (1976), mica-fish with dip opposite to the shear sense are not stable. Then, at least four solutions are possible: (i) the orientation is transient and can result from simple shear deformation in the first half of the cycle; (ii) the orientation is transient and results from deformation by transtension; (iii) the orientation is stable and is a consequence of deformation by transtension; (iv) the flow is simple shear and is channelled, and can lead to stable antithetic dips as demonstrated by Marques and Coelho (2001).

4. Conclusions

1. In natural rocks, SPOs developed in viscous simple shear flow are always transient and cyclical. In simple shear and for high R values, flats last for significantly greater γ intervals then ramps, and, thus, the probability of finding an S/C-type fabric (either syn or antithetic) is fairly high.
2. Transtension and transpression are very efficient at developing intense transient SPOs, at low γ values, whose duration depends directly on R and S_r. They are clearly more efficient than simple shear for identical values of R. In transpression and transtension, increasing S_r (or R) at constant R (or S_r) promotes a stronger SPO, at γ values progressively lower.
3. The greater the S_r in transpression, the closer the SPO becomes to the shear direction. Conversely, the greater the absolute value of Sr in transtension, the further apart the SPO becomes from the shear direction. Therefore, the SPO in transpression cannot be, in many circumstances, distinguished from the shear foliation.
4. Transpression produces, mostly, SPOs with synthetic dip, either transient or stable. When the SPO defines an S/C structure with the shear foliation, this composite fabric is always antithetic and, thus, indicates the wrong sense of shear. Transtension produces, mostly, SPOs with antithetic dip, either transient or stable. When the SPO defines an S/C structure with the shear foliation, this composite fabric is always synthetic and, thus, indicates the correct sense of shear.
5. At the end of each cycle, deformation is not perceptible from rotated particles, although shear strain can be very high, because they have spread apart and assumed orientations identical to the initial ones.
6. To use an SPO as a vorticity gauge, one must clearly demonstrate that it is not transient, i.e. its orientation corresponds to a ϕ_5.

Acknowledgements

This is a contribution to project GEOMODELS (PCTI/CTA/32742/99 and POCTI/CTA/38695/2001). S. Coelho benefited from a scholarship funded by FCT (BM/2238/2000). Reviews by S.K. Ghosh and L. Arbaret appreciably improved the quality of the paper. We also acknowledge the efficient and fair work of the editor (J. Hippertt).

References

Arbaret, L., Mancktelow, N., Burg, J.-P., 2001. Effect of shape and orientation on rigid particle orientation and matrix deformation in simple shear flow. Journal of Structural Geology 23, 113–125.

Berthé, D., Choukroune, P., Jegouzo, P., 1979. Orthogneiss, mylonites and non-coaxial deformation of granites: the example of the South Armorican shear zone. Journal of Structural Geology 1, 31–42.

Bretherton, F.P., 1962. The motion of rigid particles in a shear flow at low Reynolds number. Journal of Fluid Mechanics 14, 284–304.

Fernandez, A., Feybesse, J.L., Mezure, J.F., 1983. Theoretical and experimental study of fabrics developed by different shaped markers in two-dimensional simple shear. Bullettin de la Societé Géologique de France 25, 319–326.

Freeman, B., 1985. The motion of rigid ellipsoidal particles in slow flows. Tectonophysics 113, 163–183.

Gay, N.C., 1968. Pure shear and simple shear deformation of inhomogeneous viscous fluids. 1. Theory. Tectonophysics 5, 211–234.

Ghosh, S.K., 1977. Drag patterns of planar structures around rigid inclusions. In: Saxena, S.K., Bhattacharji, S. (Eds.), Energetics of Geologic Processes, Springer-Verlag, Berlin, pp. 94–120.

Ghosh, S.K., Ramberg, H., 1976. Reorientation of inclusions by combination of pure and simple shear. Tectonophysics 34, 1–70.

Ildefonse, B., Fernandez, A., 1988. Influence of the concentration of rigid markers in a viscous medium on the production of preferred orientations. An experimental contribution, 1. Non coaxial strain. Bulletin of the Geological Institutions of the University of Uppsala 14, 55–60.

Ildefonse, B., Mancktelow, N.S., 1993. Deformation around rigid particles: the influence of slip at the particle/matrix interface. Tectonophysics 221, 345–359.

Ildefonse, B., Launeau, P., Bouchez, J.-L., Fernandez, A., 1992a. Effect of mechanical interactions on the development of shape preferred orientations: a two-dimensional experimental approach. Journal of Structural Geology 14, 73–83.

Ildefonse, B., Sokoutis, D., Mancktelow, N.S., 1992b. Mechanical interactions between rigid particles in a deforming ductile matrix. Analogue experiments in simple shear flow. Journal of Structural Geology 14, 1253–1266.

Jeffery, G.B., 1922. The motion of ellipsoidal particles immersed in a viscous fluid. Proceedings of the Royal Society of London A 102, 161–179.

Ježek, J., 1994. Software for modeling the motion of rigid triaxial ellipsoidal particles in viscous flow. Computers & Geosciences 20, 409–424.

Ježek, J., Melka, R., Schulmann, K., Venera, Z., 1994. The behaviour of rigid triaxial particles in viscous flows—modelling of fabric evolution in a multiparticle system. Tectonophysics 229, 165–180.

Ježek, J., Schulmann, K., Segeth, K., 1996. Fabric evolution of rigid inclusions during mixed coaxial and simple shear flows. Tectonophysics 257, 203–221.

Marques, F.O., Cobbold, P.R., 1995. Development of highly non-cylindrical folds around rigid ellipsoidal inclusions in bulk simple shear: natural examples and experimental modelling. Journal of Structural Geology 17, 589–602.

Marques, F.O., Coelho, S., 2001. Rotation of rigid elliptical cylinders in viscous simple shear flow: analogue experiments. Journal of Structural Geology 23, 609–617.

Passchier, C.W., 1987. Stable positions of rigid objects in non-coaxial flow—a study in vorticity analysis. Journal of Structural Geology 9, 679–690.

Passchier, C.W., 1997. The fabric attractor. Journal of Structural Geology 19, 113–127.

Passchier, C.W., Simpson, C., 1986. Porphyroclast systems as kinematic indicators. Journal of Structural Geology 8, 831–843.

Pennacchioni, G., Di Toro, G., Mancktelow, N., 2001. Strain-insensitive peferred orientation of porphyroclast in Mont Mary mylonites. Journal of Structural Geology 23, 1281–1298.

Reed, L.J., Tryggvason, E., 1974. Preferred orientations of rigid particles in a viscous matrix deformed by pure shear and simple shear. Tectonophysics 24, 85–98.

Rosas, F.M., Marques, F.O., Luz, A., Coelho, S., 2002. Sheath folds formed by drag induced by rotation of rigid inclusions in viscous simple shear flow: nature and experiment. Journal of Structural Geology 24, 45–55.

Van den Driessche, J., Brun, J.-P., 1987. Rolling structures at large shear strain. Journal of Structural Geology 9, 691–704.

Willis, D.G., 1977. A kinematic model of preferred orientation. Geological Society of America Bulletin 88, 883–894.